Available online at www.sciencedirect.com
ScienceDirect
Journal of the European Ceramic Society 30 (2010) 839–846
www.elsevier.com/locate/jeurceramsoc

Effect of TiO_2 on the mullite formation and mechanical properties of alumina porcelain

Noemí Montoya [a], Francisco Javier Serrano [b], María Mercedes Reventós [b], José María Amigo [b], Javier Alarcón [a,*]

[a] *Department of Inorganic Chemistry, University of Valencia, Calle Dr. Moliner 50, 46100 Burjasot, Valencia, Spain*
[b] *Department of Geology, University of Valencia, Calle Dr. Moliner 50, 46100 Burjasot, Valencia, Spain*

Received 18 May 2009; received in revised form 6 October 2009; accepted 15 October 2009
Available online 13 November 2009

Abstract

The effect of adding TiO_2 to standard alumina porcelain on its microstructure and flexural strength was investigated. A series of alumina porcelain bodies containing increasing amounts of TiO_2 were prepared by extruding mixtures of raw materials and TiO_2. Porcelain rods were fired under industrial scheduling in a manufacturing kiln. The overall degree of crystalline and amorphous phase content within the porcelain bodies was quantitatively determined using a Rietveld analysis. Results indicated a higher amount of mullite formation in porcelain bodies containing TiO_2. Examination of the product materials using field emission scanning electron microscopy showed a high density of secondary mullite crystals present in the earlier feldspar grain areas of specimens with TiO_2. Energy dispersive X-ray analysis of secondary mullite crystals revealed that Ti^{4+} enters into the secondary mullite structure forming a Ti^{4+}-mullite solid solution. Assessment of the mechanical properties of the TiO_2 containing bodies indicated that small addition raises the flexural strength of the standard porcelain. The improvement in mechanical properties could be associated with an increase of both specimen density and relative content of types II and III secondary mullites. Both observations may be attributed to a decrease in the viscosity of melted feldspar grains, which in turn favours the nucleation and growth of secondary mullite crystals and thus increases the final density of porcelain bodies.

Keywords: Alumina porcelain; Titania; Microstructure; Mullite; Flexural strength

1. Introduction

Because of its insulating properties, the ceramic material alumina porcelain has important applications in the distribution and transformation of electric power. Although alumina porcelains are commonly considered as traditional ceramic materials, they are also labelled as high tech materials due to their widespread use in applications demanding high technical requirements. The two main properties exhibited by these materials are: high mechanical strength and low dielectric loss.[1] There is still considerable interest in improving the mechanical properties of alumina porcelains. It is widely assumed that the mechanical properties of ceramics are dependant on their microstructure, i.e. the quantities, sizes, size distributions, and shapes of various constituent phases. The evolution of alumina porcelain formation from a mixture of raw materials (kaolin, feldspar, alumina and small amounts of quartz) to the final product microstructure is known in general terms.[2] The gross microstructure of alumina porcelain consists of alumina, mullite and residual quartz in a glassy matrix.[3,4] It may be assumed based on results from previous reported studies that the mechanical properties of porcelain materials used for high-voltage insulators may be improved by incorporating a high corundum and low residual quartz content.[1,5]

Mullite is the only stable binary phase in the Al_2O_3–SiO_2 system. Pure mullite is a solid solution with a composition $Al_2[Al_{2+2x}Si_{2-2x}]O_{10-x}$, where $0.17 \leq x \leq 0.5$.[6,7] The compositions of the end-members of thermodynamically stable mullites are $3Al_2O_3{\cdot}2SiO_2$ ($x = 0.25$) and $2Al_2O_3{\cdot}SiO_2$ ($x = 0.40$), referred to as 3:2 and 2:1 mullites, respectively. Two main types of mullites are formed at different stages of the porcelain firing. These mullites are distinguished by their

* Corresponding author. Tel.: +34 96 3544584; fax: +34 96 3544322.
E-mail address: javier.alarcon@uv.es (J. Alarcón).

0955-2219/$ – see front matter © 2009 Elsevier Ltd. All rights reserved.
doi:10.1016/j.jeurceramsoc.2009.10.009

different morphologies and compositions. There exists the so-called primary mullite, which comes from the clay component (relict), and the secondary mullite which crystallizes from the feldspar melt.[3,4,8,9] Formation of the primary mullite occurs via transformation of the spinel-type structure phase formed from metakaolin, while the secondary mullite forms from reaction between the clay and feldspar relicts at ∼1200 °C.[10] Iqbal and Lee discovered two types of secondary mullites.[9] The first one named type-MII mullite has a granular morphology, and its crystals are shorter than those of the second type-MIII mullite. Crystals associated with the latter are highly elongated and acicular. As Iqbal and Lee stated, the observed variation in morphology may be explained by differences in gradient viscosity of the relevant matrices and subsequent, more-rapid mass transport associated with type-MIII secondary mullite. A third substance named tertiary mullite has also been found in alumina porcelains. This third type of mullite is formed at the edges of corundum crystals by dissolution and further precipitation of alumina in a SiO_2-rich matrix.

It has been hypothesized that achieving a high degree of secondary mullite interlocked structure with acicular morphology and small needle diameter may improve the mechanical properties of alumina porcelains.[10] Different additives have been used in small content to (1) lower the firing temperature, (2) favour formation of mullite and (3) improve the mechanical strength of electrical porcelains.[11–16] Basically, these additives facilitate the nucleation of acicular mullite located within an inter-phase between the clay relicts and the glass produced by the melted feldspar, and their subsequent growth into the melted feldspar grains. Thus, they function as nucleating agents for the crystallization of acicular mullite. TiO_2 has been extensively studied as a nucleating agent used in several glassy systems for the purpose of controlling crystallization in the different crystalline phases.[17–20] However, as far as we know there is no detailed information describing the effect TiO_2 has on influencing the microstructure and mechanical properties of alumina porcelain bodies.

The aim of this work is to examine the role played by the additive TiO_2 in the formation of secondary mullites in alumina porcelains. The research entails preparation and microstructural characterization of alumina porcelain bodies containing increasing amounts of TiO_2. A second objective is to monitor evolution of the flexural mechanical strength in porcelain bodies upon increasing the amount of TiO_2 and to establish a relationship between mechanical strength and secondary mullite features.

2. Experimental procedure

2.1. Preparation of porcelain samples

The composition of the reference alumina porcelain chosen for this study was 35.5 wt% ball clay, 14.5 wt% china clay, 19 wt% potassium feldspar, wt% silica sand and 26 wt% calcined alumina. A series of alumina porcelain bodies containing increasing amounts of TiO_2 were prepared by adding this mineralizer in its anatase crystalline form to the reference alumina porcelain body. The compositions of the pure and TiO_2-containing alumina porcelains prepared in this study are given in Table 1.

Table 1
Composition (in wt%) of pure and TiO_2-containing alumina porcelains.

Raw materials	Samples				
	AP0	AP2	AP4	AP6	AP8
Ball clay	35.5	34.8	34.1	33.4	32.7
China clay	14.5	14.2	13.9	13.6	13.3
Potassium feldspar	19.0	18.6	18.2	17.9	17.5
Quartz	5.0	4.9	4.8	4.7	4.6
Calcined alumina	26.0	25.5	25.0	24.4	23.9
Rutile	0.0	2.0	4.0	6.0	8.0

Each batch was prepared by dispersing raw materials in an aqueous suspension containing a high concentration of solids. The suspension was dehydrated using a filter press and the resulting cakes were extruded into cylindrical bars (10 cm length × 1 cm diameter). After drying the specimens were thermally treated in a manufacturing furnace at 1300 °C following an industrial firing schedule.

2.2. Techniques of characterization

The following techniques were used to monitor the chemical and structural changes occurring in the porcelain specimens throughout the thermal treatment.

Differential thermal analysis (Model 1700, Perkin Elmer, Norwalk, CT, USA) was carried out in air with Pt liners, and within a temperature range between 100 ° C and 1300 °C using a heating rate of 10 °C min^{-1}. Finely powdered α-Al_2O_3 served as the reference substance.

X-ray diffraction analysis (Model D-5000, Siemens, Karlsruhe, Germany) was performed using a graphite monochromatic Cu Kα radiator operating at 30 kV and 40 mA. X-ray diffraction patterns were acquired in an 8–100° (2θ°) range, with a step size of 0.02° (2θ°) and a counting time of 10 s.

The quantity of each phase present in the final alumina porcelain bodies was determined from X-ray diffraction data using a Rietveld refinement algorithm. The analysis was performed with software Fullprof98,[21] available from the software package Winplotr.[22] The internal standard used in the study was ZnO. The following parameters were incorporated during the refinement process: scale factor; zero displacement correction; unit cell parameters; peak profile parameters using a pseudo-Voight function and an overall temperature factor. The structural parameters and atomic positions for mullite,[23] quartz,[24] α-Al_2O_3,[25] rutile[26] and zincite[27] were taken from the literature.

The microstructure of thermally treated alumina porcelain bodies was observed by using field emission scanning electron microscopy (Model S-4100, Hitachi Ltd., Tokyo, Japan) operating at 30 kV. Samples were first etched with a diluted HF solution for 3 min, and subsequently washed with H_2O in order to improve the quality of the image.

Energy-dispersive X-ray analysis was performed using a scanning electron microscope (Model JSM-6300, Jeol, Oxford, England) operating at 20 kV. This instrument is equipped with an

energy dispersive X-ray spectrometer (Pentafet, Oxford Instruments, Knoxwille, TN). Specimens were mounted in a polymer resin and polished with progressively finer SiC papers. Samples were carbon coated prior to acquiring the X-ray spectra.

Flexural strength of the fired samples series containing increasing amounts of TiO_2 was measured with a universal testing machine (Model 5500R, Instron, Shakopee, MN) using a three-point loading test. A load rate of 20 kg/s was applied to specimen bars that were 10 cm in length and having a 1 cm diameter. The results reported here are the average measurements taken over 20 test pieces per each body. Bulk densities of the fired samples were determined using the conventional liquid displacement method.

3. Results and discussion

3.1. Transformations during the heating of electrical alumina porcelain bodies

Three peaks are observed in the DTA curves obtained for the TiO_2 containing porcelain samples upon heating them to 1300 °C. The first and second endothermic peaks appear at around 100 °C and 560 °C. These 2 peaks correspond to the vaporisation of absorbed water and the dehydroxylation of kaolinite, respectively. The last broad peak originates from an exothermic effect centred at around 985 °C, and is associated with the metakaolinite to alumina-silica spinel transformation.[28] The first mullite formed originates from clay relicts, by the transformation of the alumina-spinel phase at temperatures above 1000 °C and appears as aggregates of small crystals (<0.5 μm). This mullite is referred to as the primary mullite.[4,29] It may be concluded from the studies carried out on the TiO_2-containing porcelain specimen series that (1) only transformations taking place on heating kaolinite, present in the clay component of porcelain specimens, produce some thermal effects and (2) the temperature at which changes are produced is independent of the amount of titanium dioxide present. It may also be noted that there were no specific thermal effects detected during the crystallization of secondary mullite from the feldspar raw material.

Dense, sintered alumina porcelain bodies were prepared by thermally processing extruded bars containing increasing amounts of TiO_2 in a manufacturing furnace with an industrial heating schedule and at a final temperature of 1300 °C. X-ray diffraction patterns of the final bodies are displayed in Fig. 1. According to the diffractograms acquired for the thermally processed alumina porcelain bodies, three crystalline phases including α-Al_2O_3, mullite and quartz are detected in all specimens. Also rutile is present in compositions containing TiO_2. However, part of the nominal titanium oxide content is evidently incorporated into a crystalline phase forming a solid solution and/or into the amorphous phase.

3.2. Microstructural characterization of TiO_2-containing electrical porcelains

In order to establish a relationship between the microstructure and mechanical properties of the alumina porcelain bodies the amount of crystalline phases present for specimens examined and their corresponding microstructures, i.e. relative distribution, size and shape of the different constituent phases was determined. A second goal of the research was to validate the incorporation of TiO_2 (as Ti^{4+}) into the secondary mullite crystals.

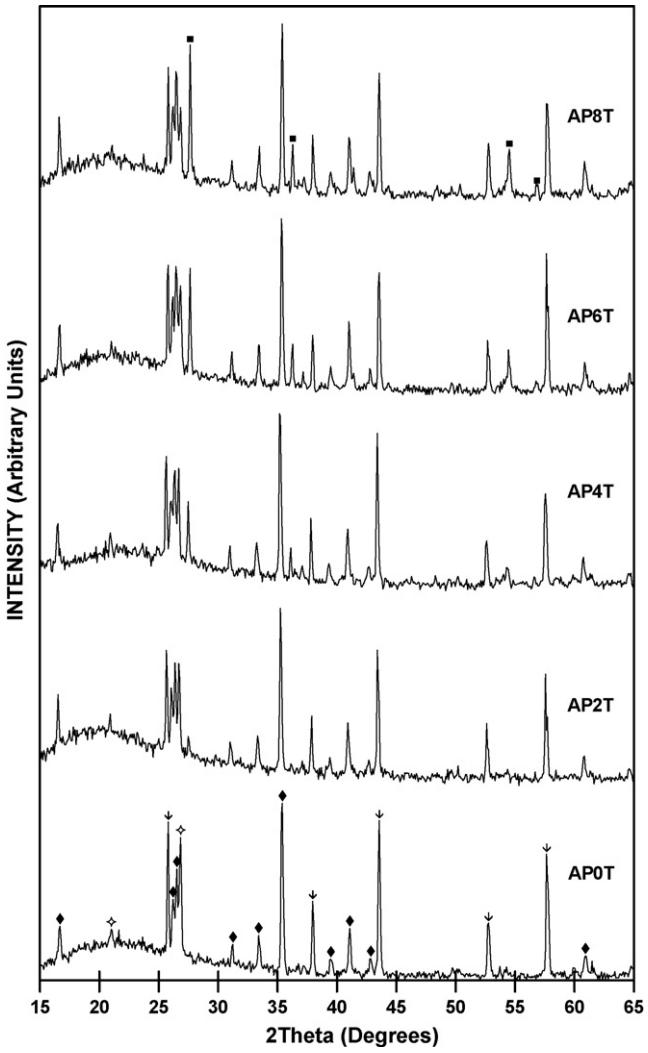

Fig. 1. XRD patterns of a series of industrially thermally processed alumina porcelain bodies series with increasing TiO_2 content (♦ is mullita, ↓ is alumina, ✧ is quartz and ■ is rutile).

3.2.1. Quantitative phase analysis of heated porcelains

The relative quantities of the different phases present in the series of TiO_2-containing porcelain final products were determined by a Rietveld analysis. The accuracy and precision of this technique as used for the quantitative determination of phases has been verified for multicomponent (polyphasic) materials.[30] The results obtained for the porcelain sample series fired under the industrial scheme are shown in Table 2. Also some details of the Rietveld refinement procedure are included. The final Rietveld plot for the specimen AP2, shown as representative, is given in Fig. 2. The results indicate that addition of titanium dioxide is accompanied by an increase in the amount of mullite

Table 2
Results for the quantitative analysis (wt%) and details of the Rietveld refinement for alumina porcelain bodies thermally treated under industrial conditions.

	AP0	AP2	AP4	AP6	AP8
α-Al_2O_3	25.9 ± 0.5	24.2 ± 0.4	22.2 ± 0.5	21.6 ± 0.4	20.8 ± 0.4
Quartz	5.5 ± 0.2	4.6 ± 0.2	2.7 ± 0.2	3.6 ± 0.2	2.9 ± 0.2
Mullite	22.0 ± 0.7	27.0 ± 0.7	25.7 ± 0.8	27.4 ± 0.7	28.9 ± 0.8
Glassy phase	46.6 ± 0.9	43.4 ± 0.9	47.1 ± 0.9	43.7 ± 0.9	41.4 ± 0.9
Rutile	0.0	0.7 ± 0.1	2.4 ± 0.2	3.7 ± 0.2	6.1 ± 0.2
R_p (%)[a]	5.61	5.81	6.24	6.27	6.36
R_{wp} (%)[a]	7.48	7.68	8.30	8.09	8.35
R_{wp} (expected) (%)[a]	5.32	5.35	5.37	5.45	5.52
χ^2	1.98	2.07	2.39	2.20	2.29

[a] The R_{exp}, R_p and R_{wp} are the discrepancy factors that characterize quality of fit.

formed for all compositions. Likewise, a slight decrease in the amount of quartz present occurs as a result of increasing the amount of TiO_2 in fired porcelain batches. It is to be noted that for the composition AP6, the amount of TiO_2 detected as unreacted rutile is 3.7 wt%. So, the amount of TiO_2 dissolved in the crystalline phases, mainly mullite, and/or into the glassy phase is ∼2.3 wt%. Rutile is the stable form of TiO_2. Also, unreacted anatase transforms during the thermal treatment into rutile.

The incorporation of TiO_2 into the mullite structure of specimens prepared using a variety of methods has been previously reported by others.[31–33] The reported results suggests that the amount of Ti^{4+} soluble into the $3Al_2O_3{\cdot}2SiO_2$ mullite is ∼4.0 wt% TiO_2. Recently, by using a sol–gel technique of preparation we have confirmed this result and found that for the Al_2O_3-rich mullites, $2Al_2O_3{\cdot}SiO_2$, the amount of dissolved TiO_2 is slightly higher ∼4.2 wt% TiO_2.[33]

Based on these results and comments it can be surmised that the TiO_2 plays an effective role in the crystallization of mullite in alumina porcelain bodies. In order to prove the effect this mineralizer has on determining the final properties of alumina porcelain bodies, it was necessary to (1) check if the content of both types of mullites is increased by the presence of TiO_2, and (2) verify if and how the microstructure of the final porcelain bodies is modified by the addition of small amounts of this mineralizer.

3.2.2. *Morphological and compositional features of mullite crystalline phases*

Although small changes in the size of the quartz grains occur as a result of dissolution during the thermal processing in industrial kiln, mainly for compositions with the larger nominal TiO_2 content, focus here is given to changes that take place in the mullite crystals. As mentioned above, primary mullite comes from the clay components, mainly from kaolinite, while the secondary mullite originates from melted feldspar. Considering the nature of the transformation process of kaolinite to primary mullite, it can be assumed that this transformation is not strongly influenced by the presence of TiO_2.[34] It is reasonable therefore, to assume that the mineralizer exerts an influential effect on the amount formed and characteristic features associated with the so-called secondary mullite. The amount of total mullite formed increases upon adding TiO_2, as evidenced by the results from the Rietveld analysis. Although it is not possible to quantitatively determine the size and density of secondary mullite crystals in the former feldspar grains because of the complex microstructure of porcelain bodies, a qualitatively comparison of the characteristics pertaining to secondary mullite areas for specimens with and without TiO_2 may be made. It is obvious that the area size depends primarily on the particle size distribution of the feldspar raw material. It is therefore important to perform a qualitative check for variation in the density of mullite crystals in the early feldspar grains when TiO_2 is added to the porcelain body. Figs. 3–5 show a general view of the microstructure of alumina porcelain bodies containing 0, 2 and 6 wt% TiO_2, respectively, subjected to an industrial heating schedule. Figs. 6a, 7a and 8a, show the morphological characteristics of the primary mullite and Figs. 6b, 7b and 8b display the corresponding ones for the secondary mullites in the same alumina porcelain specimens. From these figures one can see that larger acicular secondary mullite crystals and denser mullite crystal areas are more evident in the composition containing 2 wt% TiO_2 than in the pure porcelain. Therefore the formation of larger amounts of secondary mullites must be favoured by the presence of TiO_2 particles. As stated by Iqbal and Lee the secondary mullite forms by reaction between the clay relicts and feldspar relicts at ∼1200 °C[9] when the feldspar grains are melted. Therefore, the formation of crystals of secondary mul-

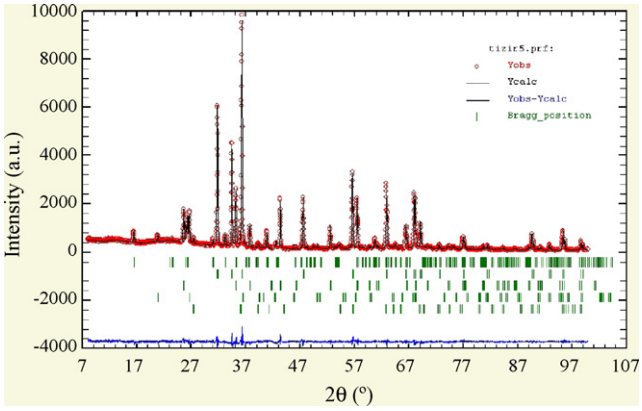

Fig. 2. Rietveld plot of the alumina porcelain AP2 heated under an industrial schedule. The calculated pattern is compared with observed data. The small vertical bars indicate the position of allowed *h k l* reflections. The difference between the observed and calculated profiles is shown in the lower trace plotted below the diffraction pattern.

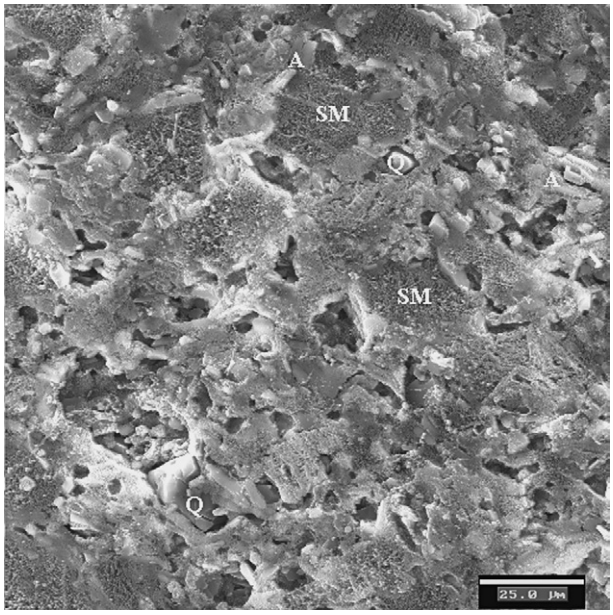

Fig. 3. FESEM micrograph of the pure alumina porcelain body AP0 (bar = 25 μm).

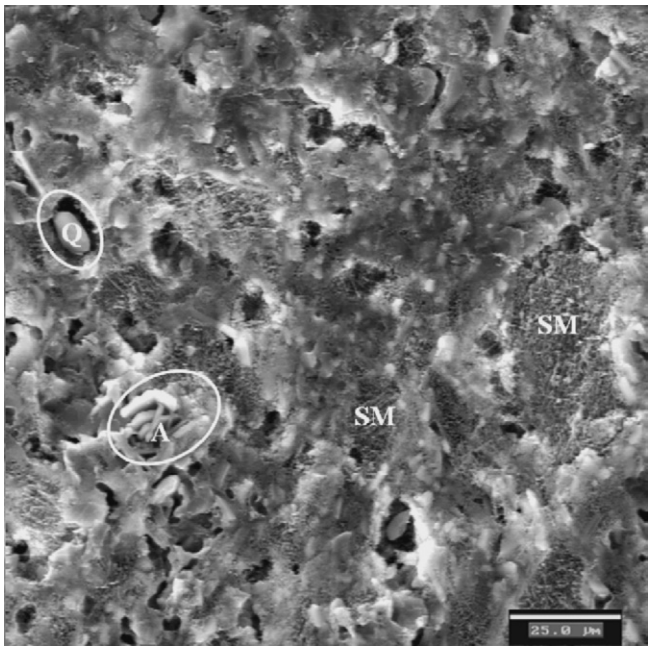

Fig. 5. FESEM micrograph of the alumina porcelain body AP6 (bar = 25 μm).

lite begins at the contact area between primary mullite crystals and feldspar melted grains. The role of the mineralizer TiO_2 can be understood if one considers that a decrease in viscosity must take place in the contact area between clay relicts, TiO_2 and feldspar melted grains. As a result of this decrease in viscosity the nucleation of secondary mullite is favoured. The effect of TiO_2 on the viscosity of SiO_2-rich glasses was previously reported by Sugai and Somiya.[35] Once nucleation of the secondary mullite has occurred its growth is also favoured because again the viscosity of the melted feldspar is lower. Thus, large crystals of secondary mullite types II and III are formed.

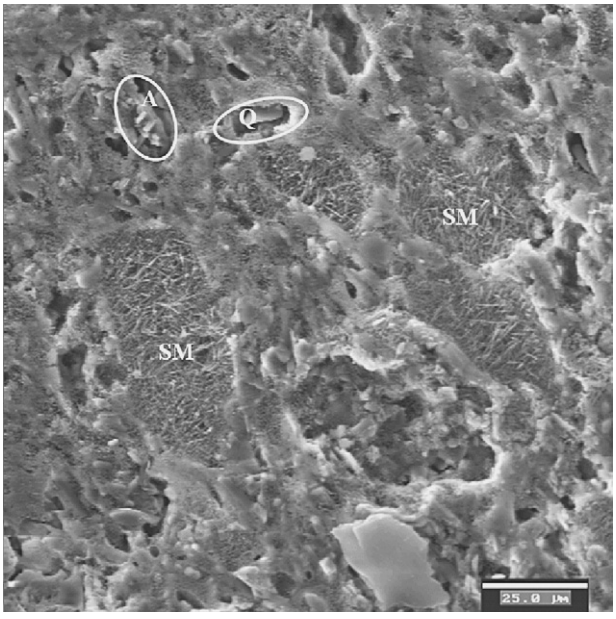

Fig. 4. FESEM micrograph of the alumina porcelain body AP2 (bar = 25 μm).

The main characteristics of the different types of mullites generated in alumina porcelain bodies upon the addition of TiO_2 may be clearly observed in Figs. 6–8. As seen in these figures, the primary mullite crystals are shorter than 250 nm whereas types II and III secondary mullites are longer than 7.5 μm. Moreover, type III secondary mullite crystals are thicker than 0.8 μm. From viewing the micrographs it may be concluded that the presence of small amounts of TiO_2 favours the formation of secondary mullites in alumina porcelain. Both the number and the size of secondary mullite crystals are enhanced. A very similar behaviour has been reported by Hong and Messing for alumina-silica diphasic gels doped with TiO_2.[36,37] They found that additions of up to 5 wt% TiO_2 produce an anisotropic growth of mullite crystals and that large mullite crystals are formed upon heating. Since the technique of preparation used by the authors is not a highly reactive one, a large amount of TiO_2 does not incorporate into the mullite structure and remains unreacted. This results in a low viscosity glassy phase that facilitates the growth of mullite crystals. The same behaviour was observed in this study when TiO_2 was added to porcelain bodies. Since the TiO_2 grains do not react appreciably with the primary mullite, they remain unreacted up to temperatures of approximately 1200 °C, which is the temperature at which the feldspar grains melt. At this temperature some amount of TiO_2 is dissolved in the glassy phase from feldspar grains where it reduces the viscosity. Subsequently, the secondary mullite is nucleated in the interface between the glassy phase and the outer surface of the clay relicts (i.e. primary mullite). After nucleation, the growth of mullite crystals occurs inside the melted feldspar grains.

In order to estimate the relative content of Ti^{4+} in the secondary mullite crystals as a function of the distance from the interface where nucleation starts, energy dispersive X-ray spectroscopy was performed as a spot analysis. This was accom-

plished by stopping and carefully positioning the electron beam on the point to be analysed, which was selected on the SEM screen during display of the image. The TiO_2 content of secondary mullite crystals longer than 10 μm, such as the ones shown in Fig. 7b, remains almost constant, and varies within the ranges 1.7–1.1 and 1.2–0.9 wt% TiO_2, at the ends close to the nucleation interface and at the opposite crystal ends, respectively. It is evident that titanium oxide is incorporated into the mullite crystals even in cases where starting amounts of TiO_2 are nominal (as small as 2 wt%). Some level of inaccuracy should be assumed when interpreting the data since the microanalyses were performed on polished and etched samples. Nevertheless, the results support incorporation of a relatively large amount of TiO_2 into the secondary mullite.

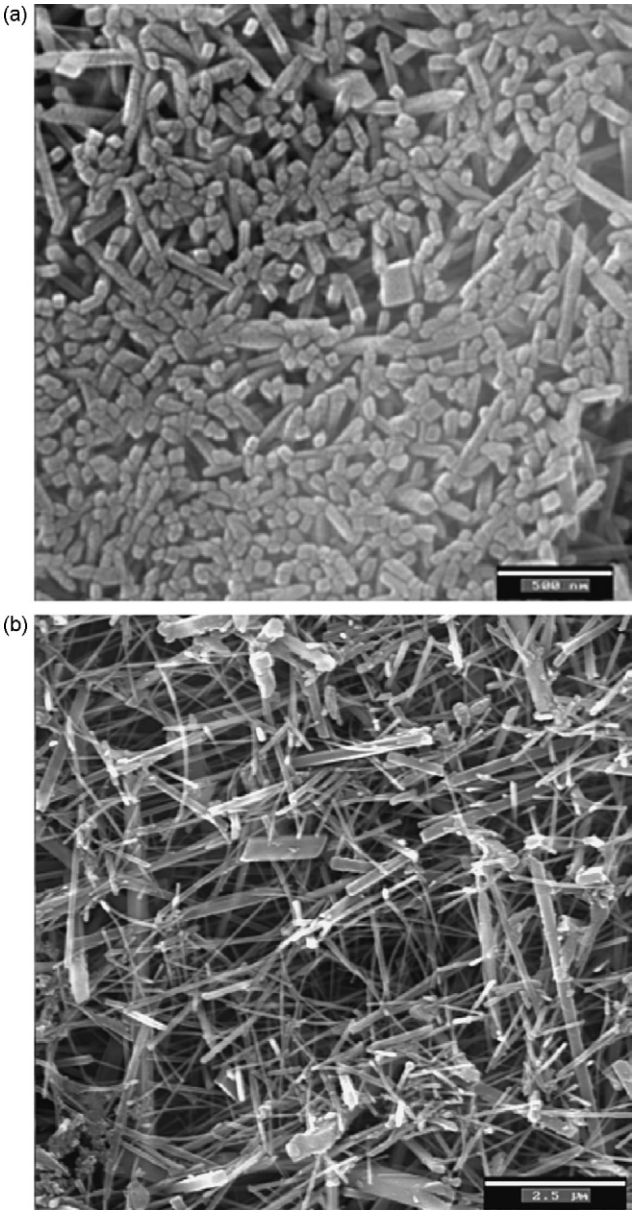

Fig. 6. High magnification view of mullite crystals in alumina porcelain AP0: (a) primary (bar = 500 nm); (b) secondary of types II and III (bar = 2.5 μm).

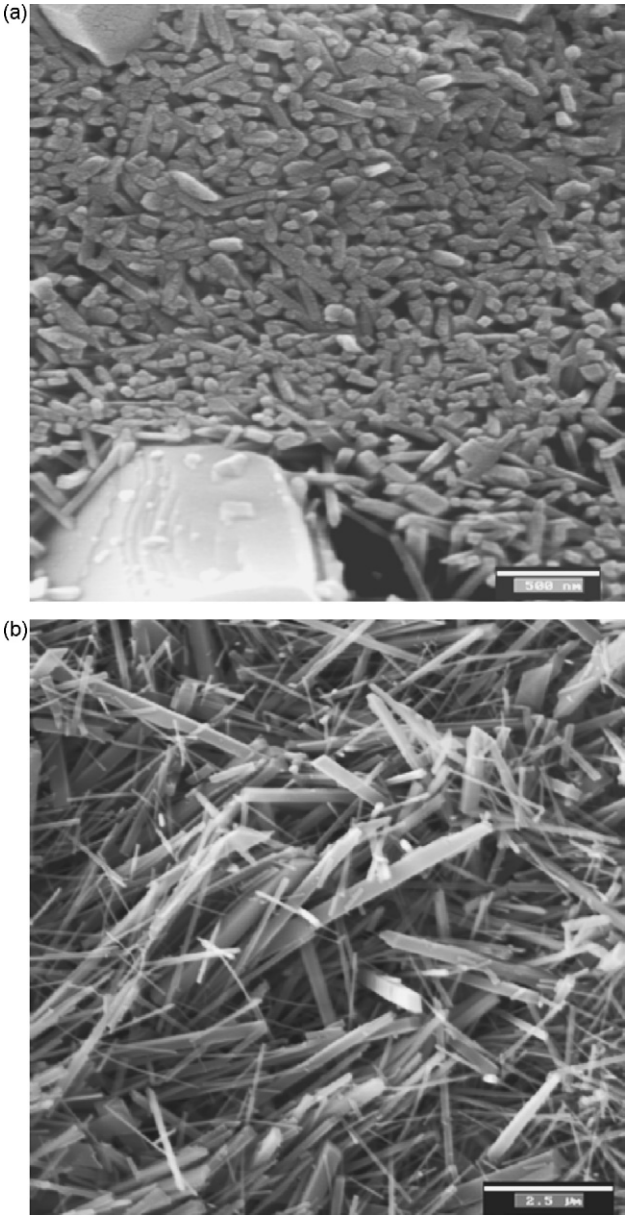

Fig. 7. High magnification view of mullite crystals in alumina porcelain AP2: (a) primary (bar = 500 nm); (b) secondary of types II and III (bar = 2.5 μm).

3.3. Relationship between microstructure and flexural strength of specimens

Fig. 9 shows the flexural strength and bulk density variations observed for the series of fired porcelains containing increasing amounts of TiO_2. The addition of titanium oxide yields an increase in bulk density for all heated alumina porcelain bodies. An increased resistance is also observed upon adding small amounts (2 wt%) of TiO_2. This mechanical feature remains almost constant when higher levels of mineralizer are present. Both the increase in the mullite content and the increase in density arising from addition of TiO_2 contribute to this behaviour. Furthermore, the morphological characteristics of types II and III secondary mullites products are also favorable for improving mechanical properties. As can be seen in the FESEM

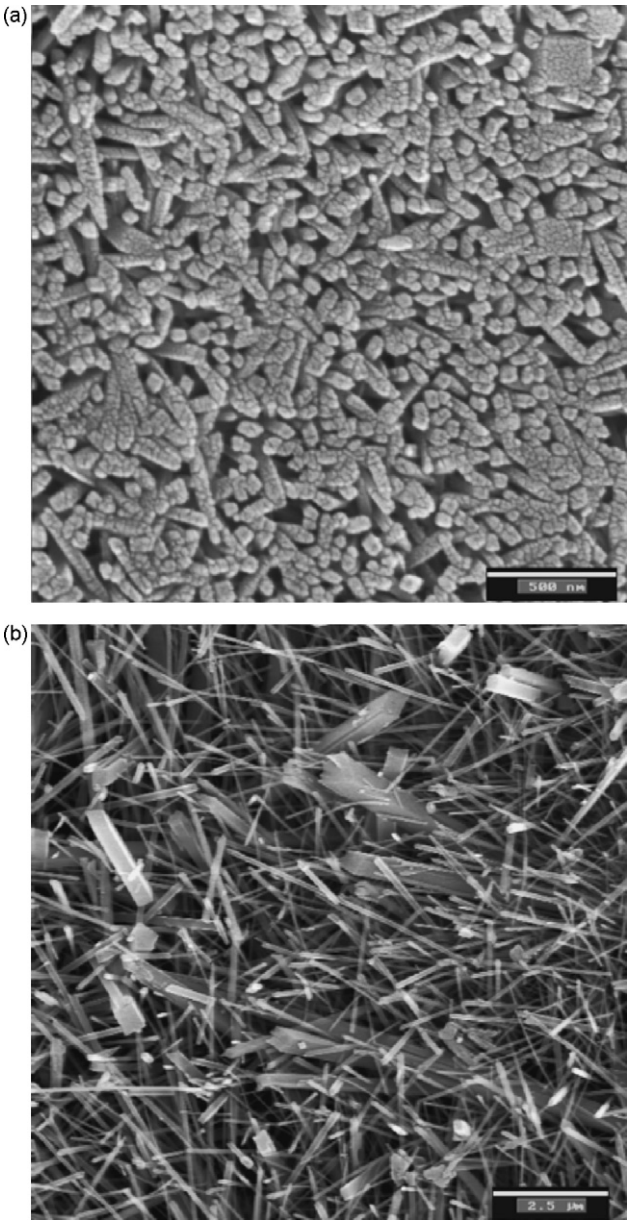

Fig. 8. High magnification view of mullite crystals in alumina porcelain AP6: (a) primary (bar = 500 nm); (b) secondary of types II and III (bar = 2.5 μm).

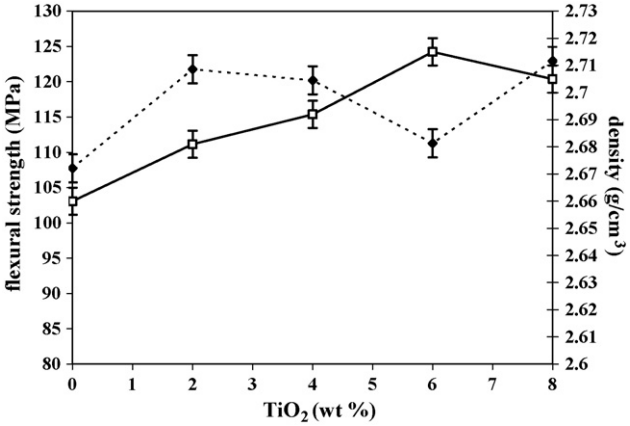

Fig. 9. Flexural strength (♦) and bulk density (□) variations of alumina porcelains with increasing amount of TiO_2.

micrographs of secondary mullites (Figs. 4–8), more homogeneous size crystals are formed in bodies having lower titanium oxide content while for bodies with higher TiO_2 content, for example the body AP6, an almost bimodal thickness distribution of mullite crystals is observed. In this example, very thin as well as thick secondary mullite crystals are displayed (Fig. 8b). There is a notable decrease in flexure strength accompanying specimens containing 6 wt% TiO_2 compared to that of other bodies containing less TiO_2. The decrease in flexural strength observed for this composition is unexpected since it is characterized by the highest bulk density and also has a high amount of crystalline mullite: but may be due to specific microstructural features of mullite secondary crystals developed for this amount of TiO_2.

4. Conclusions

The effect adding TiO_2 to standard alumina porcelain on its microstructure and flexural strength while processed under an industrial heating schedule was studied. Results from quantitative X-ray diffraction and field emission scanning electron microscopy experiments show that TiO_2 promotes the crystallization of both types II and III secondary mullites. The role of the TiO_2 mineralizer located at the interface between the melted feldspar grains, the TiO_2 particles and the clay relicts is to reduce the viscosity of the melt and subsequently favour mass-transport. TiO_2 was incorporated into secondary mullite crystals. Improvement in the mechanical features of alumina porcelains realized with small additions of titanium oxide could be explained by the accompanying increases in both the amount of secondary mullite and density in the final body and the microstructural characteristics of the formed secondary mullite.

References

1. Liebermann, J., Avoiding quartz in alumina porcelain for high-voltage insulators. Part I. *Am. Ceram. Soc. Bull.*, 2001, **80**, 37–42.
2. Lee, W. E. and Rainforth, W. M., *Ceramic Microstructures*. Chapman and Hall, London, UK, 1994, p. 256.
3. Lundin, S. T., Electron microscopy of Whiteware bodies. In *Transactions of the IV International Ceramic Congress*, 1954, pp. 383–390.
4. Schüller, K. H., Reaction between mullite and glassy phase in porcelains. *Trans. Br. Ceram. Soc.*, 1964, **63**, 103–117.
5. Liebermann, J., Avoiding quartz in alumina porcelain for high-voltage insulators, Part II. *Am. Ceram. Soc. Bull.*, 2001, **80**, 43–48.
6. Cameron, W. E., Mullite a substituted alumina. *Am. Mineral.*, 1977, **62**, 747–755.
7. Angel, R. J. and Prewitt, C. T., Crystal structure of mullite: a re-examination of the average structure. *Am. Mineral.*, 1986, **71**, 1476–1482.
8. Iqbal, Y. and Lee, W. E., Fired porcelain microstructures revisited. *J. Am. Ceram. Soc.*, 1999, **82**, 3584–3590.
9. Iqbal, Y. and Lee, W. E., Microstructural evolution in triaxial porcelain. *J. Am. Ceram. Soc.*, 2000, **83**, 3121–3127.
10. Carty, W. M. and Senapati, U., Porcelain-raw materials, processing, phase evolution, and mechanical behaviour. *J. Am. Ceram. Soc.*, 1998, **81**, 3–20.
11. Chaudhuri, S. P., Influence of mineralizers on the constitution of hard porcelain. I. Mineralogical compositions. *Am. Ceram. Soc. Bull.*, 1974, **53**, 169–171.
12. Chaudhuri, S. P., Influence of mineralizers on the constitution of hard porcelain. II. Microstructures. *Am. Ceram. Soc. Bull.*, 1974, **53**, 251–254.

13. Tasic, Z. D., Improving the microstructural and physical-properties of alumina electrical porcelain with Cr_2O_3, MnO_2 and ZnO additives. *J. Mater. Sci.*, 1993, **28**, 5693–5701.
14. Naga, S. M., Sallam, E. H., El-Didamony, H. and Aziz, D. O. A., Aluminous electrical porcelain doped with Ba^{2+}. *Ind. Ceram.*, 1997, **17**, 149–152.
15. Tkalcec, E., Prodanovic, D., Falz, W. and Hennicke, H. W., Microstructure and properties of aluminous electrical porcelain doped with $BaCO_3$. *Trans. J. Br. Ceram. Soc.*, 1985, **84**, 94–98.
16. Alarcón, J., Guillem, C. and Guillem, M. C., Action of calcium carbonate as mineralizer of porcelain bodies for casting. *Interceram*, 1984, **4**, 37–39.
17. Zdaniewski, W., DTA and X-ray analysis study of nucleation and crystallization of $MgO–Al_2O_3–SiO_2$ glasses containing ZrO_2, TiO_2 and CeO_2. *J. Am. Ceram. Soc.*, 1975, **58**, 163–169.
18. Partridge, G., An overview of glass ceramics. Part 1. Development and principal bulk applications. *Glass Technol.*, 1994, **35**, 116–127.
19. Stewart, D. R., TiO_2 and ZrO_2 as nucleants in a lithia aluminosilicate glass–ceramics. In *Advances in Nucleation and Crystallization in Glasses*, ed. L. L. Hench and S. W. Freman. American Ceramic Society, Columbus, OH, 1971, pp. 83–90.
20. Torres, F. J. and Alarcón, J., Microstructural evolution in fast-heated cordierite-based glass-ceramic glazes for ceramic tile. *J. Am. Ceram. Soc.*, 2004, **87**, 1227–1232.
21. Rodriguez-Carvajal, J., A program for Rietveld refinement and pattern matching analysis. In *Abstracts of the Satellite Meeting on Powder Diffraction*, 1990, p. 127.
22. Rodriguez-Carvajal, J. and Roisnel, T., Fullprof98 and Winplotr: New Windows 95/NT applications for diffraction. *Commission for Powder Diffraction*. International Union of Crystallography, 1998, p. 25, Newsletter n°. 20.
23. Balzar, D. and Ledbetter, H., Crystal structure and compressibility of 3-2 mullite. *Am. Mineral*, 1993, **78**, 1192–1196.
24. Gualtieri, A. F., Accuracy of XRPD QPA using the combined RIR method. *J. Appl. Cryst.*, 2000, **33**, 267–278.
25. Kirfel, A. and Eichhorn, K., Accurate structure–analysis with synchrotron radiation. The electron density in Al_2O_3 and Cu_2O. *Acta Cryst. A*, 1990, **46**, 271–284.
26. Gesenhues, U. and Rentscheer, T., Crystal growth and defect structure of Al^{3+}-doped rutile. *J. Solid State Chem.*, 1999, **143**, 210–218.
27. Albertsson, J. S., Abrahams, C. and Kvick, A., Atomic displacement, anharmonic thermal vibration, expansivity and pyroelectric coefficient thermal dependences in zone. *Acta Cryst. B*, 1989, **45**, 34–40.
28. Okada, K., Otsuka, N. and Ossaka, J., Characterization of spinel phase formed in the kaolin-mullite thermal sequence. *J. Am. Ceram. Soc.*, 1986, **69**, C251–C253.
29. Comer, J. J., Electron microscopy studies of mullite development in fired kaolinites. *J. Am. Ceram. Soc.*, 1960, **43**, 378–384.
30. Yasukawa, K., Terashi, Y. and Nakayama, A., Crystalline analysis of glass–ceramics by the Rietveld method. *J. Am. Ceram. Soc.*, 1998, **81**, 2978–2982.
31. Murthy, M. K. and Hummel, F. A., X-ray study of the solid solution of TiO_2, Fe_2O_3, and Cr_2O_3 in mullite ($3\,Al_2O_3{\cdot}2\,SiO_2$). *J. Am. Ceram. Soc.*, 1960, **43**, 267–273.
32. Schneider, H., Transition metal distribution in mullite. In *Mullite and Mullite Matrix Composites*, ed. S. Somiya, R. F. Davis and J. A. Pask. American Ceramic Society, Westerville, OH, 1990, pp. 135–157.
33. Ruiz de Sola, E., Serrano, F. J., Delgado-Pinar, E., Reventós, M. M., Pardo, A. I., Kojdecki, M. A., Amigó, J. M. and Alarcón, J., Solubility and microstructural development of TiO_2-containing $3Al_2O_3{\cdot}2SiO_2$ and $2Al_2O_3{\cdot}SiO_2$ mullites obtained from single-phase gels. *J. Eur. Ceram. Soc.*, 2007, **27**, 2647–2654.
34. Chaudhuri, S. P., Induced mullitization of kaolinite—a review. *Trans. Ind. Ceram. Soc.*, 1977, **76**, 113–120.
35. Sugai, M. and Somiya, S., Measurement of density, viscosity and surface tension of the melt of the system $SiO_2–TiO_2–Al_2O_3$ at 1600 °C. *Yogyo Kyokaishi*, 1982, **90**, 262–269.
36. Hong, S. H. and Messing, G. L., Mullite transformation kinetics in P_2O_5-,TiO_2-, and B_2O_3-doped aluminosilicate gels. *J. Am. Ceram. Soc.*, 1997, **80**, 1551–1559.
37. Hong, S. H. and Messing, G. L., Anisotropic grain growth in diphasic-gel-derived titania-doped mullite. *J. Am. Ceram. Soc.*, 1998, **81**, 1269–1277.